

ORIGINAL RESEARCH

Open Access



Imaging bone turnover assessment through volumetric density-adjusted standardized uptake value using quantitative bone SPECT/CT in osteoporosis

Dong Yun Lee¹ , Jungsu S. Oh¹ , Ji Wan Kim² , Seung Hun Lee³ , Beom-Jun Kim³ , Jung-Min Koh³ , Jae Seung Kim¹ and Jin-Sook Ryu^{1*}

Abstract

Background Serum bone turnover markers offer limited insight into metabolic activity at the individual vertebra level in osteoporosis. This study introduces a novel image-derived bone turnover marker for individual vertebrae to address this limitation, utilizing volumetric density-adjusted quantitative bone single-photon emission computed tomography/computed tomography (SPECT/CT) with [^{99m}Tc]Tc-DPD. This retrospective study included 177 lumbar vertebrae from 55 postmenopausal South Korean women. The mean standardized uptake value (SUV_{mean} , g/cm³) and volumetric bone mineral density (vBMD, mg/cm³) were determined within a 2-cm³ volume of interest in the trabecular portion of each vertebra using quantitative SPECT and CT. The density-adjusted mean standardized uptake value ($dSUV_{mean}$) was calculated by dividing the SUV_{mean} by the vBMD and multiplying by 1,000.

Results SUV_{mean} correlated positively with vBMD ($r = 0.60$, $p < 0.001$). Conversely, $dSUV_{mean}$ correlated negatively with vBMD ($\rho = -0.66$, $p < 0.001$), highlighting the inverse relationship between bone mass and turnover after density adjustment of SUV_{mean} . Patients with major osteoporotic fractures had lower vBMD (62.5 ± 29.4 vs. 92.3 ± 27.4 mg/cm³, $p = 0.001$) but higher $dSUV_{mean}$ (100.8 ± 60.7 vs. 62.6 ± 17.5 , $p = 0.001$) compared to those without fractures, reinforcing the association between fracture prevalence, low bone mass, and high bone turnover.

Conclusion Volumetric density-adjusted quantitative bone SPECT/CT offers a novel image-derived bone turnover marker for assessing bone turnover in osteoporosis. This method provides a precise assessment of fragility at the individual vertebra level, which may enhance personalized osteoporosis management.

Keywords Quantitative bone SPECT/CT, Standardized uptake value, Bone turnover marker, Volumetric bone density, Quantitative CT

*Correspondence:

Jin-Sook Ryu
jsryu2@amc.seoul.kr

¹Department of Nuclear Medicine, Asan Medical Center, University of Ulsan College of Medicine, Seoul, Republic of Korea

²Department of Orthopedic Surgery, Asan Medical Center, University of Ulsan College of Medicine, Seoul, Republic of Korea

³Department of Internal Medicine, Division of Endocrinology and Metabolism, Asan Medical Center, University of Ulsan College of Medicine, Seoul, Republic of Korea

Background

The incidence of osteoporosis and the associated socio-economic burden of osteoporotic fracture have increased worldwide due to the aging population [1]. The primary goal of osteoporosis treatment is to minimize fracture risk and prevent subsequent fragility fractures, especially among high-risk individuals [2]. Thus, there is a high demand for accurate assessment of bone strength-related fracture risk.

Although bone mineral density (BMD), typically measured by dual-energy X-ray absorptiometry (DXA), is a crucial determinant of fracture risk, higher bone mass does not entirely eliminate fracture risk [3–5]. This has led to growing recognition of “bone quality” as an integral aspect of bone strength, distinct from bone mass. Bone quality encompasses various factors, including bone turnover, microarchitecture, mineralization, and micro-damage [6–8]. Among them, several parameters provide quantitative indicators of bone turnover. Although bone histomorphometry is considered the gold standard for measuring bone turnover [9], it is invasive and not widely used. As a result, serum bone turnover markers (sBTMs), which include bone formation and bone resorption markers, are favored in clinical practice due to their simplicity and cost-effectiveness [8]. However, sBTMs offer a cumulative measure of whole-body bone turnover, lacking the specificity needed for individual bone assessment.

Bone scintigraphy using bone-seeking radiopharmaceuticals has been extensively used to track active bone turnover and metabolism [10]. These radiopharmaceuticals bind to hydroxyapatite in bone tissue, reflecting osteoblastic activity and mineralization rates [11]. However, traditional bone scintigraphy produces two-dimensional images primarily subject to visual analysis, limiting their quantitative utility. Recent advancements in imaging technology, particularly the introduction of hybrid single-photon emission computed tomography/computed tomography (SPECT/CT) system, have enabled three-dimensional scintigraphic imaging [12]. This allows for precise quantification of radiotracer activity and provides accurate anatomical information [13, 14]. CT-based attenuation correction in SPECT offers quantitative turnover rate, such as standardized uptake value (SUV), similar to those in static PET. Additionally, the CT component provides bone density information in Hounsfield units (HU), comparable to quantitative CT (QCT) and BMD measurements [15, 16].

Clinically, bone SPECT/CT is valuable for differentiating the cause of lower back pain and for quantitative analysis [17]. Previous studies have attempted to quantify bone turnover in the lumbar spine (L-spine) using a volume of interest (VOI) approach [18–20]. These studies facilitated direct comparison with BMD and showed a positive relationship between SUV and L-spine bone

density parameters. However, this contradicts the established inverse correlation between bone turnover and bone mass [21, 22], suggesting that SUV alone may not accurately reflect bone turnover, similar to sBTMs.

The avidity of bone-seeking radiotracer at active bone turnover sites is influenced by the available bone surface or volume for tracer uptake [23, 24]. Since bone formation rate per unit of bone surface or volume equates to bone turnover by histomorphometry definitions [9], further dimensional or volumetric adjustment of SUV is necessary for accurate normalization of turnover rates in individual vertebrae. Given that BMD influences tracer accumulation, we hypothesize that normalizing SUV by BMD, rather than using SUV alone, could more accurately reflect the bone turnover rate at these sites. In this context, our study explores the feasibility of using volumetric bone mineral density (vBMD)-adjusted SUV from quantitative bone SPECT/CT as a novel marker for bone turnover. We aimed to elucidate its significance by correlating it with the osteoporosis-related parameters.

Methods

Patient selection

We retrospectively recruited postmenopausal women who underwent both bone SPECT/CT of the L-spine and DXA within a three-month interval from May 2017 to August 2021 after excluding males and pre-menopausal women. Following the International Society for Clinical Densitometry recommendations [25], post-menopausal women with at least two vertebrae suitable for quantification without compression fractures, degenerative changes, or spinal implants were included. A comprehensive review of electronic medical records and radiologic images was conducted to assess clinical characteristics as outlined in the Fracture Risk Assessment Tool (FRAX), including the presence of prevalent major osteoporotic fractures (MOF) in the hip, spine, radius, or humerus. The 10-year probability of a MOF or hip fracture was calculated using the South Korean reference available on the FRAX website (www.sheffield.ac.uk/FRAX). Reasons for undergoing bone SPECT/CT were also identified. This study was approved by the Institutional Review Board (IRB No. 2020–1061) of our institution, and the need for informed consent was waived.

Bone SPECT/CT acquisition protocol and quantitative image analysis

All patients underwent whole-body planar scintigraphy at least three hours after an intravenous injection of approximately 740 MBq (20 mCi) of [^{99m}Tc]Tc-labeled 3,3-diphosphono-1,2-propanodicarboxylic acid ([^{99m}Tc]Tc-DPD). Data including patients' body weight and height, initial and residual radioactivity before and after injection, and the timing of radioactivity measurements

were recorded for precise dose calculation after decay correction. SPECT/CT images of the L-pine and/or pelvis were acquired using a hybrid SPECT/CT camera (Symbia Intevo 16, Siemens). For quantification, the ^{99m}Tc activity was cross-calibrated between the dose calibrator and SPECT scanner. SPECT images were acquired over 360° using a step-and-shoot mode with 45 frames per detector head view, each lasting 22 s, and non-circular orbit. A non-enhanced CT scan was subsequently acquired with 110 kV and 40-reference mAs using adaptive dose modulation (CARE Dose 4D) and a slice thickness of 2 mm. Images were reconstructed to generate

attenuation-corrected SPECT data using the xSPECT-Bone™ reconstruction algorithm (Siemens) with 1 subset and 24 iterations, enabling post-processed image quantification with a 256×256 matrix size.

For quantitative analysis, the body weight-based mean standardized uptake value (SUV_{mean} , g/cm^3) and mean HU (HU_{mean}) of each vertebra from the first (L1) to the fourth (L4) lumbar vertebrae were measured by dedicated software (Syngo Via, Siemens). A 2 cm^3 spherical VOI was drawn in the trabecular center of each vertebra, avoiding cortical bone and the basivertebral vein (Fig. 1a).

The SUV_{mean} equation was as follows:

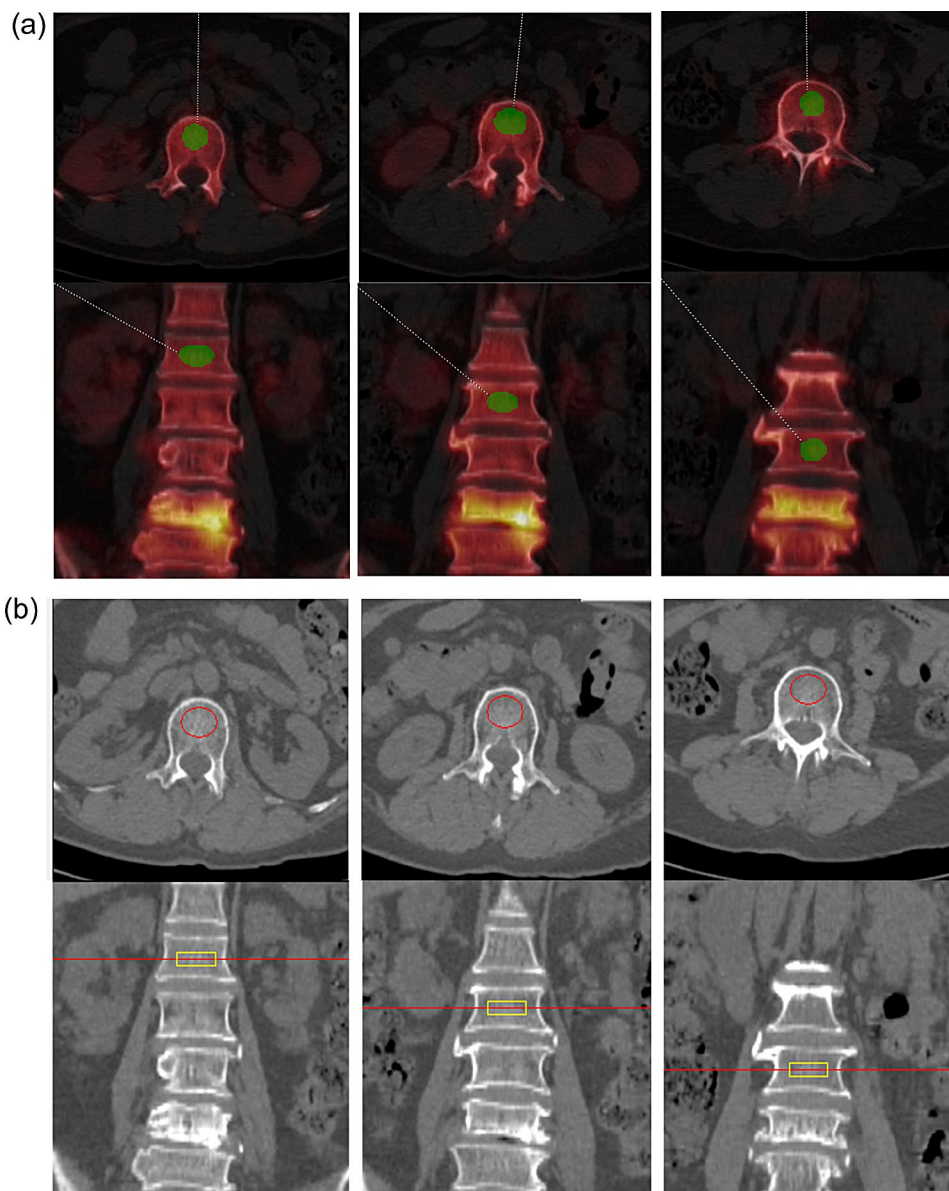


Fig. 1 Representative images of the quantitation in measurable and non-measurable vertebra. **(a)** Example of measuring the HU_{mean} and SUV_{mean} parameters using a 2 cm^3 spherical volume of interest (VOI) from L-spine SPECT/CT in one shot by a dedicated software. The image show axial and sagittal views with the green VOI placed in the measurable trabecular center of each L1–L3 body, while the non-measurable L4 body, with vertebral wedging and active degenerative changes, is also presented. **(b)** Example of measuring bone density parameters from QCT using a 2 cm^3 cylindrical VOI in the same area as **(a)**

$$SUV_{mean} (g/cm^3) = \frac{\text{Mean radioactivity concentration in the volume of interest of tissue (MBq/cm}^3)}{\text{Injected dose (MBq)/Patient's body weight (g)}}$$

QCT measurement

Using the CT component of SPECT/CT, we analyzed the vBMD (mg/cm^3) for the same vertebral bodies retrospectively using QCT Pro (Mindways Software Inc.), with asynchronous phantom-based calibration. A cylindrical VOI equivalent to 2 cm^3 was semi-automatically placed in the trabecular center of each vertebra and manually adjusted to avoid cortical bone and the basivertebral vein (Fig. 1b).

Deriving image-based bone turnover parameters

Given that trabecular bones in the vertebrae exhibit higher turnover rates than cortical bones and are crucial in determining the response to anti-osteoporotic medication [26], adopting nearly simultaneous VOIs from SPECT and QCT for density adjustment is ideal for assessing bone turnover. We derived an additional variable, bone density-adjusted SUV_{mean} ($dSUV_{mean}$), by multiplying 1,000 by SUV_{mean} and then dividing the vBMD in each vertebra:

$$dSUV_{mean} = \frac{SUV_{mean} (g/cm^3) \times 1,000}{vBMD (mg/cm^3)}$$

Similarly, HU-adjusted SUV_{mean} ($hSUV_{mean}$) was calculated by multiplying 1,000 by SUV_{mean} and then dividing by HU_{mean} :

$$hSUV_{mean} (g/cm^3) = \frac{SUV_{mean} (g/cm^3) \times 1,000}{HU_{mean}}$$

DXA acquisition and image analysis

Areal BMD (aBMD, g/cm^2) from L1 to L4 was measured using DXA equipment (GE Lunar Prodigy Advance). The region of interest (ROI) was automatically generated by the equipment's software and manually adjusted by a skilled technologist when necessary. Trabecular bone score (TBS) was retrospectively analyzed from L-spine DXA scans using iNsight software version 3.0 (Med-Imaps) with the ROI corresponding to those designated for BMD measurement.

Statistical analysis

Descriptive statistics, expressed as mean \pm standard deviation, were used to summarize the baseline characteristics of the study population. Pearson's (r) or Spearman's correlation coefficients (ρ) were employed for patient- and vertebra-based analyses to examine relationships between variables. In the patient-based analysis,

measured values from L1 to L4 were averaged to create a single representative value per patient. Partial correlation coefficients were additionally used to adjust for potential confounding factors. Group comparisons were conducted using the Mann–Whitney U test. A p -value of <0.05 was considered statistically significant. All analyses were performed using SPSS version 23.0 (IBM Corp.).

Results

Baseline demographics

Figure 2 presents the patients' recruitment process. After excluding males, pre-menopausal women, and those with non-quantifiable vertebrae, 55 postmenopausal women with at least two measurable vertebrae were included in the study. Among them, 24 patients (43.6%) had prevalent MOF. The baseline characteristics of the patients are summarized in Table 1. The majority (45/55, 81.8%) underwent SPECT/CT due to low back or hip pain. Nine patients (16.3%) had a history of glucocorticoid intake, and 25 patients (45.5%) exhibited clinical features suggestive of secondary osteoporosis, such as diabetes mellitus, Parkinson's disease, or were on anticoagulation therapy. A total of 177 intact vertebrae were included in the quantitative analysis.

Comparison of SPECT/CT, DXA, and QCT parameters

The average value (mean \pm SD) of SUV_{mean} , HU_{mean} , and vBMD from SPECT/CT for all patients was $5.2 \pm 1.3\text{ g/cm}^3$, 99.1 ± 39.9 , and $79.3 \pm 31.7\text{ mg/cm}^3$, respectively. The aBMD, T-score, and TBS values from DXA were $0.90 \pm 0.14\text{ g/cm}^2$, -2.1 ± 1.1 , and 1.4 ± 0.1 , respectively. Both patient- and vertebra-based analyses demonstrated a very strong correlation between HU_{mean} from SPECT/CT and vBMD from QCT ($r=0.99$, $p<0.001$; $r=0.99$, $p<0.001$, respectively; Supplementary Fig. 1a and 2a) and a moderate-to-weak correlation between HU_{mean} from SPECT/CT and aBMD from DXA ($r=0.47$, $p<0.001$; $r=0.36$, $p<0.001$). Additionally, $dSUV_{mean}$ and $hSUV_{mean}$ showed a very strong correlation ($r=0.98$, $p<0.001$; $r=0.97$, $p<0.001$; Supplementary Fig. 1b and Fig. 2b).

SUV_{mean} showed a strong positive correlation with HU_{mean} ($r=0.60$, $p<0.001$; $r=0.60$, $p<0.001$) and vBMD ($r=0.60$, $p<0.001$; $r=0.60$, $p<0.001$) and a weak positive correlation with aBMD ($r=0.25$, $p=0.062$; $r=0.20$, $p=0.009$), indicating that higher bone density was generally associated with SUV_{mean} . However, TBS showed no significant relationship with SUV_{mean} ($r=0.18$, $p=0.18$; $r=0.12$, $p=0.20$), as depicted in Fig. 3.

Conversely, $dSUV_{mean}$ showed a strong negative correlation with HU_{mean} ($\rho = -0.69$, $p<0.001$; $\rho = -0.66$, $p<0.001$), vBMD ($\rho = -0.69$, $p<0.001$; $\rho = -0.66$, $p<0.001$) and a moderate or weak negative correlation with aBMD ($\rho = -0.43$, $p<0.001$; $\rho = -0.36$, $p<0.001$; Fig. 4). Interestingly, inverse correlations in exponential functions between $dSUV_{mean}$ and density parameters

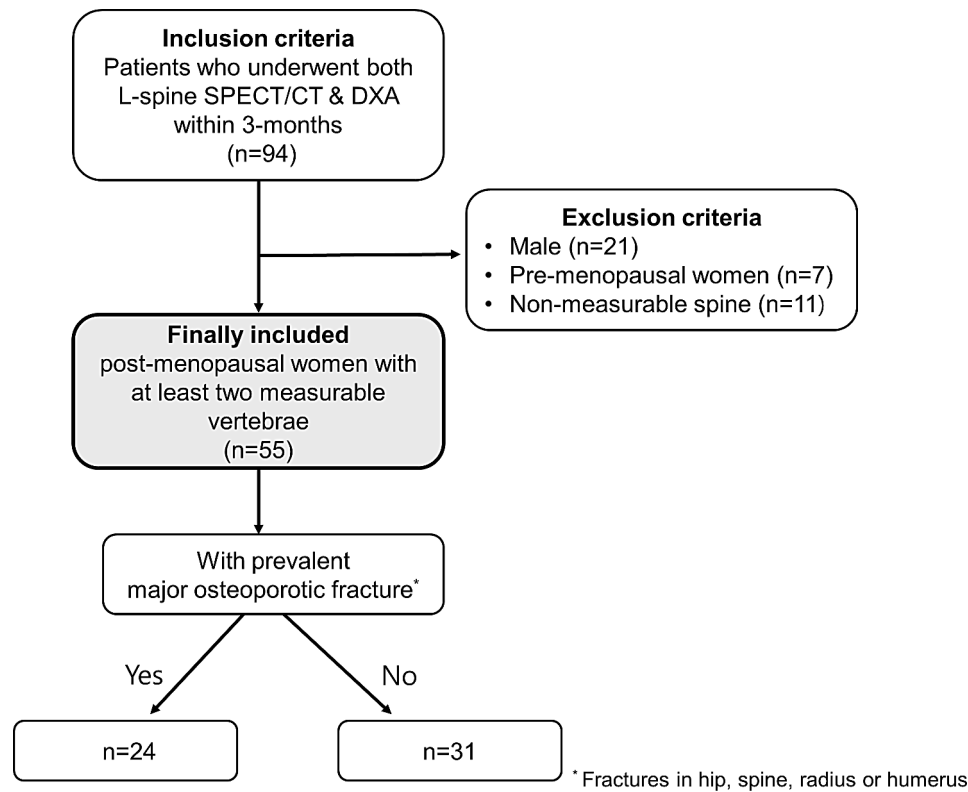


Fig. 2 Flow chart of patient selection

Table 1 Baseline characteristics of the patients

Characteristics	Values (n=55)
Included number of vertebrae	177
Interval between DXA and SPECT/CT (days)	18±25 (median, 7; range, 0–90)
Reasons for bone SPECT/CT	
- Low back/hip pain	45
- Fracture	5
- Avascular necrosis of the femur	4
- Ankylosing spondylitis	1
Injected dose of [^{99m} Tc]Tc-DPD (mCi)	20.4±0.9
SPECT/CT acquisition time after injection (min)	223.9±21.3
Age (years)	66.2±8.3
Height (cm)	155.1±6.3
Weight (kg)	57.6±8.5
BMI (kg/m ²)	24.0±3.4
Clinical features related with osteoporosis	
- Smoking	0
- Alcohol intake	1
- Glucocorticoid intake	9 (16.3%)
- Rheumatoid arthritis	4 (7.2%)
- Secondary osteoporosis	25 (45.5%)
- Osteoporosis drug intake	21 (38.2%)

Presented numbers are means±standard deviation, or proportion in percent, respectively

DXA=dual-energy X-ray absorptiometry; ^{99m}Tc-DPD=^{99m}Tc-labeled 3,3-diphosphono-1,2-propanodicarboxylic acid; BMI=body mass index

(aBMD, vBMD) were observed regardless of fracture history, and these trends remained significant even after adjusting for age and BMI, as indicated in Table 2. The dSUV_{mean} showed a weak-to-very weak negative correlation with TBS ($\rho = -0.37, p=0.006; \rho = -0.18, p=0.047$).

Comparison of image-derived parameters and clinical factors

In terms of age, there was a moderate negative correlation with both SUV_{mean} ($r=-0.44, p=0.001$) and vBMD ($r=-0.59, p<0.001$), whereas dSUV_{mean} showed a weak positive correlation ($r=0.34, p=0.01$). BMI did not show any significant correlation with these parameters. Compared with patients without MOF (Table 3), those with prevalent MOF were older (69.6±9.9 years vs. 63.5±5.8 years, $p=0.012$) and had a higher 10-year probability of MOF (13.1±6.4% vs. 7.4±3.5%, $p<0.001$) and hip fractures (5.2±4.2% vs. 2.2±2.1%, $p<0.001$) according to FRAX. They also tended to lower HU_{mean} (78.9±38.0 vs. 114.7±34.3, $p=0.001$), lower vBMD (62.5±29.4 mg/cm³ vs. 92.3±27.4 mg/cm³, $p=0.001$), lower aBMD (0.85±0.16 g/cm² vs. 0.93±0.11 g/cm², $p=0.010$), and lower TBS (1.34±0.06 vs. 1.38±0.09, $p=0.019$), but higher dSUV_{mean} (100.8±60.7 vs. 62.6±17.5, $p=0.001$) and hSUV_{mean} (84.6±59.8 g/cm³ vs. 50.6±14.7 g/cm³, $p=0.004$) as seen in Fig. 5, while SUV_{mean} did not show significant difference (5.0±1.4 g/cm³ vs. 5.5±1.2 g/cm³).

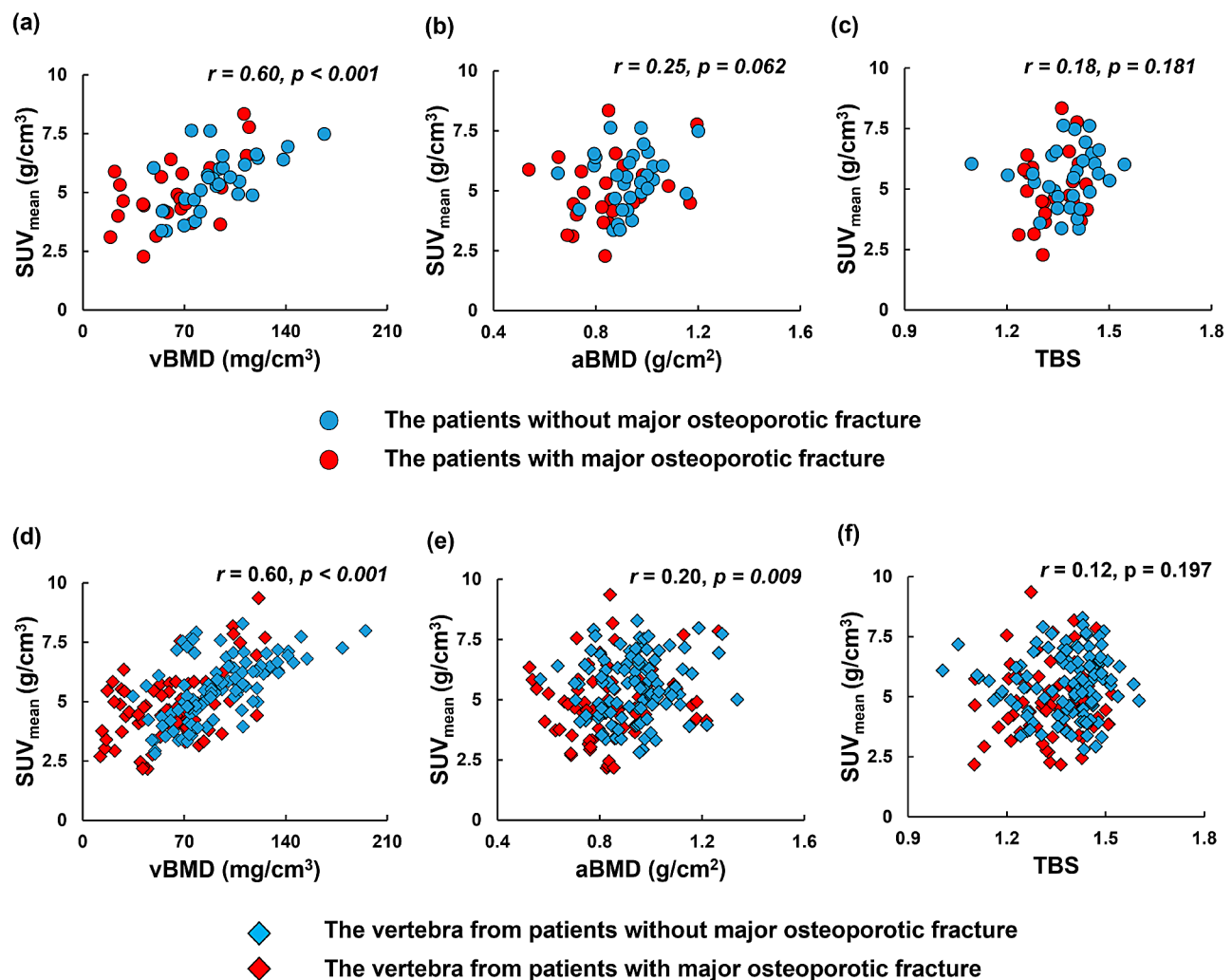


Fig. 3 The graphs show the correlations of SUV_{mean} with vBMD, aBMD, and TBS using Pearson's correlation coefficient. Panels (a-c) represent the patient-based analysis, and panel (d-f) represent the vertebra-based analysis

cm³, $p=0.131$). After adjusting for age and BMI, vBMD ($r=-0.35, p=0.011$) and $dSUV_{mean}$ ($\rho=0.33, p=0.017$) remained significantly associated with the presence of MOFs, while SUV_{mean} ($r=-0.03, p=0.83$) did not demonstrate such a relationship.

Discussion

In this study, we introduced a novel image-based parameter of bone turnover, the equivalent vBMD-adjusted SUV_{mean} ($dSUV_{mean}$), using quantitative bone SPECT/CT. Our findings revealed an inverse correlation between $dSUV_{mean}$ and bone density parameters, supporting the established concept that a high bone turnover rate correlates with lower bone mass. In contrast to previous studies and our findings, which showed a positive correlation between SUV_{mean} and bone density parameters [18–20], SUV_{mean} appears to be more influenced by bone mass. On the other hand, $dSUV_{mean}$ serves as an indicator of

turnover rate per unit density, offering a novel perspective distinct from SUV_{mean} . These findings underscore the importance of adjusting SUV for bone density to accurately assess bone turnover.

Our findings align with prior research that utilized [¹⁸F]NaF PET for evaluating bone turnover [23, 27, 28]. Frost et al. normalized bone turnover by using DXA-derived bone mineral apparent density (BMAD)-corrected net fluoride uptake, demonstrating higher turnover in osteopenic and osteoporotic groups compared to the normal group [23]. These findings are consistent with our observations, emphasizing the importance of density adjustment for accurate bone turnover assessment. However, BMAD remains a surrogate measure [29], whereas our study utilized direct vBMD measurements from the same VOI, providing more precise data. Additionally, the dynamic [¹⁸F]NaF PET approach has practical

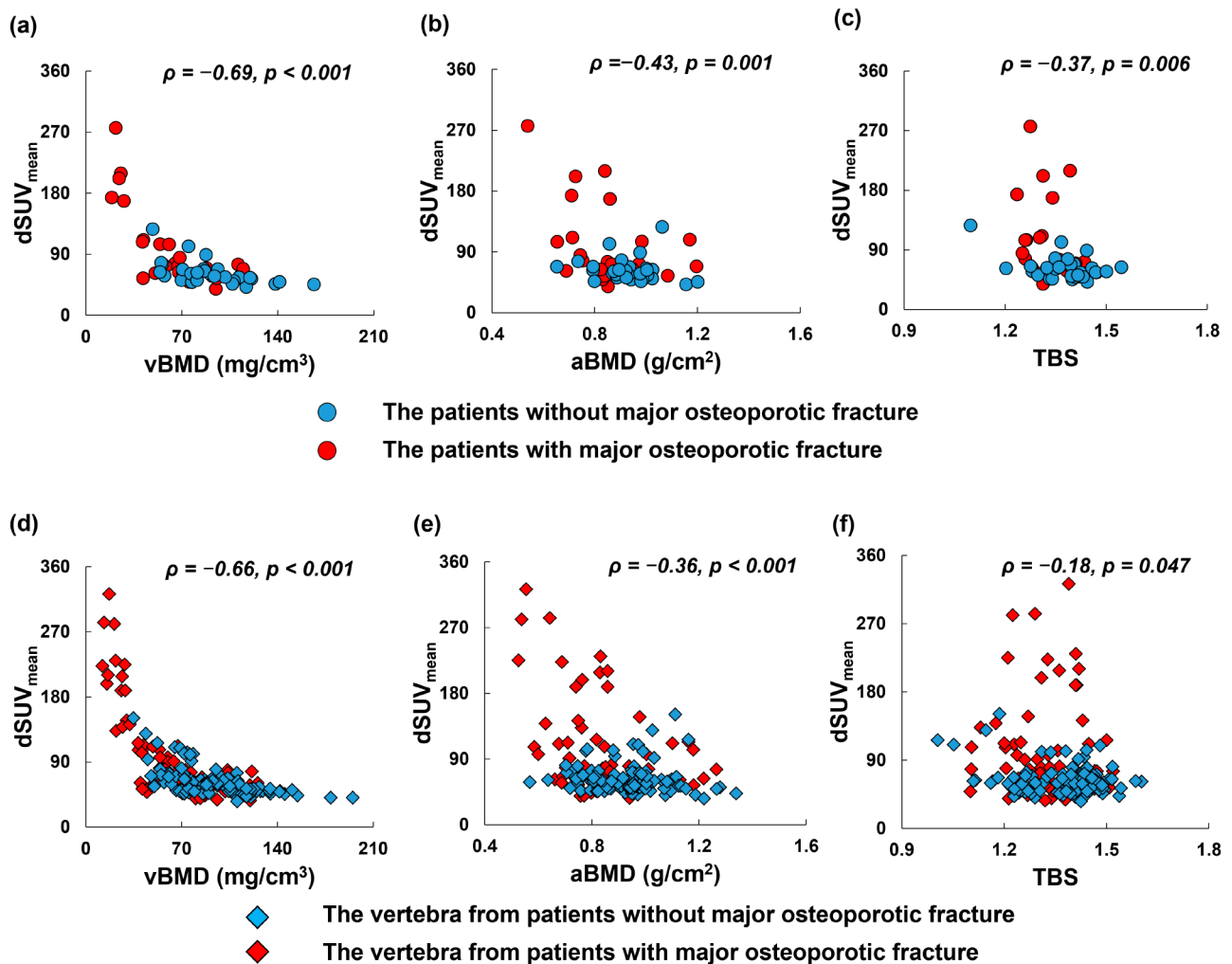


Fig. 4 The graphs show the correlations of $dSUV_{mean}$ with vBMD, aBMD, and TBS using Spearman’s correlation coefficient. Panels (a-c) represent the patient-based analysis, and panel (d-f) represent the vertebra-based analysis

Table 2 Partial correlation coefficients among quantitative parameters of bone strength corrected for age and BMI

Coefficients	aBMD	vBMD	SUV_{mean}	$dSUV_{mean}$
aBMD	1.0			
vBMD	0.54**	1.0		
SUV_{mean}	0.18	0.47**	1.0	
$dSUV_{mean}$	-0.41**	-0.64**	0.16	1.0

**Significance at the 0.01 level

BMI=body mass index; aBMD=areal bone mineral density; vBMD=volumetric bone mineral density; SUV_{mean} = mean standardized uptake value; $dSUV_{mean}$ = bone density-adjusted SUV_{mean}

limitations, including extended acquisition time and the necessity for input function.

Our study expands the foundational SPECT-only works of Front et al. [30] and Israel et al. [31]. They demonstrated the potential of SPECT for quantifying bone metabolism but lacked the precision offered by CT integration. Key advancements in our methodology include

improved quantitation accuracy through CT-based attenuation correction and density adjustment, higher resolution for defining a region of interest in the trabecular bone with detailed anatomical information from CT, and the use of advanced algorithms, such as xSPECT-Bone™, for more reliable value, SUV.

Our approach of adjusting SUV for vBMD using quantitative bone SPECT/CT is cost-effective and efficient. Unlike usual static SUV measurement [32], which assumes a soft tissue density of approximately $1 g/cm^3$, our method corrects for the inherent differences in bone density. This adjustment is crucial for accurately reflecting bone turnover. However, static bone SPECT/CT measurements face challenges such as partial volume effects, non-specific tracer binding, and signal noise, which must be considered.

The inverse relationships between the $dSUV_{mean}$ and density parameters (aBMD or vBMD) mirror those

Table 3 Comparison of parameters between the groups upon MOF

Parameters	With MOF (n=24)	Without MOF (n=31)	p-value
Included number of vertebrae	3.0±0.8	3.4±0.8	0.080
Interval between DXA and SPECT/CT (days)	13.7±23.8	20.9±25.6	0.109
SPECT/CT start time after injection (min)	226.5±17.9	222.0±23.6	0.259
Age (years)	69.6±9.9	63.5±5.8	0.012*
Height (cm)	155.1±6.3	156.0±6.0	0.255
Weight (kg)	57.6±8.5	59.3±7.8	0.066
BMI (kg/m ²)	24.0±3.4	24.4±3.1	0.377
Smoking	0	0	1.00
Alcohol intake	0	1	0.379
Glucocorticoid intake	5 (20.8%)	4 (12.9%)	0.435
Rheumatoid arthritis	3 (12.5%)	1 (3.2%)	0.193
Secondary osteoporosis	11 (45.8%)	14 (45.2%)	0.961
Osteoporosis drug intake	12 (50.0%)	9 (29.0%)	0.116
10-year probability of MOF (%)	13.1±6.4	7.4±3.5	<0.001**
10-year probability of hip fracture (%)	5.2±4.2	2.2±2.1	<0.001**
T-score of L-spine	-2.48±1.25	-1.73±0.92	0.006**
aBMD of L-spine (g/cm ²)	0.85±0.16	0.93±0.11	0.010*
vBMD of L-spine (mg/cm ³)	62.5±29.4	92.3±27.4	0.001**
aBMD of femur neck (g/cm ²)	0.71±0.09	0.78±0.11	0.057
TBS	1.34±0.06	1.38±0.09	0.019*
SUV _{mean} (g/cm ³)	5.0±1.4	5.5±1.2	0.131
HU _{mean}	78.9±38.0	114.7±34.3	0.001**
dSUV _{mean}	100.8±60.7	62.6±17.5	0.001**
hSUV _{mean} (g/cm ³)	84.6±59.8	50.6±14.7	0.004**

Presented numbers are means±standard deviation, or proportion in percent, respectively

**Significance at the 0.01 and *significance at the 0.05 level

MOF= major osteoporotic fracture; DXA=dual-energy X-ray absorptiometry; BMI=body mass index; aBMD=areal bone mineral density; vBMD=volumetric bone mineral density; TBS=trabecular bone score; SUV_{mean} = mean standardized uptake value; HU_{mean} = mean Hounsfield unit; dSUV_{mean} = density-adjusted SUV_{mean}; hSUV_{mean} = HU-adjusted SUV_{mean}

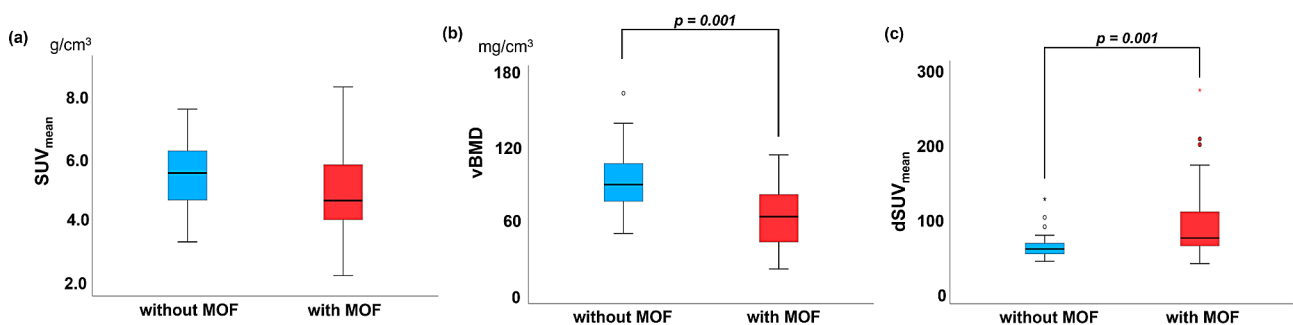


Fig. 5 The graphs show the differential values of SUV_{mean} (a), vBMD (b) and dSUV_{mean} (c) in patient-based analysis according to the major osteoporotic fractures (MOF) status. Box plots display the median, interquartile range, and outliers

between sBTM and bone strength parameters [21, 22]. The significant inverse correlation between dSUV_{mean} and vBMD aligns with the established non-linear relationship between fracture risk and bone density [33], suggesting dSUV_{mean} could serve as a potential new biomarker, or imaging bone turnover marker (iBTM). Further research is needed to explore the characteristics of iBTM and its potential clinical applications, such as diagnosing metabolic bone diseases, predicting fracture risk in osteoporosis, and monitoring therapy efficacy [34].

Patients with prevalent MOF exhibited traits similar to those noted in prior studies, such as lower BMD, TBS, and advanced age [35], alongside lower SUV_{mean} and higher dSUV_{mean}, supporting the link between high bone turnover, low bone mass, and spinal fractures [36].

Previous studies often used inconsistent VOIs that included the cortical bone and/or basivertebral vein [18–20]. In contrast, we exclusively measured SUV from the trabecular center, using a VOI nearly identical to

conventional QCT [15], likely resulting in more accurate density adjustment.

Quantitative L-spine SPECT/CT has significant opportunistic value for osteoporosis screening, offering one-shot information on bone density and quality-related markers [37, 38]. However, precise radioactivity measurement, standardized image acquisition, and accurate quantitative data from both SPECT and CT components are essential prerequisites for this application [39].

This study has limitations, including a small sample size of postmenopausal Asian women, limiting the generalizability of the results. Future research should establish normal SUV values with a coefficient of variance according to radiotracer, age, sex, and race. Additionally, due to the retrospective nature of this study, we could not compare $dSUV_{mean}$ with sBTM. Finally, the semi-automatic VOI drawing limited the representation to a restricted trabecular area in the spine. A more refined VOI encompassing the entire trabecular area would be preferable [40].

Conclusion

Volumetric density-adjusted quantitative bone SPECT/CT offers a novel image-derived bone turnover marker for assessing bone turnover in osteoporosis, providing a precise assessment of fragility at the individual vertebra level, which may enhance personalized osteoporosis management.

Abbreviations

SPECT/CT	Single-photon emission computed tomography/computed tomography
iBTM	Imaging bone turnover marker
sBTM	Serum bone turnover marker
DXA	Dual-energy X-ray absorptiometry
TBS	Trabecular bone score
QCT	Quantitative computed tomography
aBMD	Areal bone mineral density
vBMD	Volumetric bone mineral density
SUV_{mean}	Mean standardized uptake value
$dSUV_{mean}$	Bone density-adjusted mean standardized uptake value
$hSUV_{mean}$	Hounsfield unit-adjusted mean standardized uptake value

Supplementary Information

The online version contains supplementary material available at <https://doi.org/10.1186/s13550-024-01137-y>.

Supplementary Material 1

Acknowledgements

Not applicable.

Author contributions

DYL and JR contributed to the study conception and design. DYL and JWK were responsible for recruiting the patient. DYL and JSO were responsible for the quantitative analyses and the statistical analyses. DYL and JR drafted the manuscript. DYL, JSO, JWK, SHL, BK, JK, JSK and JR contributed to the interpretation of the data. DYL, JSO, JWK, SHL, BK, JK, JSK and JR critically reviewed and approved the final manuscript.

Funding

This research was supported by a grant of the Korea Health Technology R&D Project through the Korea Health Industry Development Institute (KHIDI), funded by the Ministry of Health & Welfare, Republic of Korea (grant number: HR18CO016).

Data availability

The datasets generated during and/or analysed during the current study are available from the corresponding author on reasonable request.

Declarations

Ethical approval

This study was also approved by the Institutional Review Board (IRB No. 2020–1061) of Asan Medical Center. All procedures involving human participants were in accordance with the ethical standards of the institutional and/or national research committee and with the 1964 Helsinki declaration and its later amendments or comparable ethical standards.

Consent to participate

The need for informed consent was waived by the IRB.

Competing interests

The authors declare no competing interests.

Received: 10 July 2024 / Accepted: 12 August 2024

Published online: 25 August 2024

References

1. Mohd-Tahir NA, Li SC. Economic burden of osteoporosis-related hip fracture in Asia: a systematic review. *Osteoporos Int.* 2017;28:2035–44. <https://doi.org/10.1007/s00198-017-3985-4>.
2. Nih Consensus Development Panel on Osteoporosis, Prevention D, Therapy. Osteoporosis prevention, diagnosis, and therapy. *JAMA.* 2001;285:785–95. <https://doi.org/10.1001/jama.285.6.785>.
3. Aleksova J, Kurniawan S, Elder GJ. The trabecular bone score is associated with bone mineral density, markers of bone turnover and prevalent fracture in patients with end stage kidney disease. *Osteoporos Int.* 2018;29:1447–55. <https://doi.org/10.1007/s00198-018-4468-y>.
4. Choi YJ, Lee HY, Yoon D, Kim A, Shin YS, Park HS, et al. Trabecular bone score is more sensitive to Asthma Severity and Glucocorticoid Treatment Than Bone Mineral density in asthmatics. *Allergy Asthma Immunol Res.* 2019;11:343–56. <https://doi.org/10.4168/air.2019.11.3.343>.
5. Leslie WD, Aubry-Rozier B, Lamy O, Hans D, Manitoba Bone Density P. TBS (trabecular bone score) and diabetes-related fracture risk. *J Clin Endocrinol Metab.* 2013;98:602–9. <https://doi.org/10.1210/jc.2012-3118>.
6. Gnudi S, Ripamonti C, Gualtieri G, Malavolta N. Geometry of proximal femur in the prediction of hip fracture in osteoporotic women. *Br J Radiol.* 1999;72:729–33. <https://doi.org/10.1259/bjr.72.860.10624337>.
7. Hans D, Goertzen AL, Krieg MA, Leslie WD. Bone microarchitecture assessed by TBS predicts osteoporotic fractures independent of bone density: the Manitoba study. *J Bone Min Res.* 2011;26:2762–9. <https://doi.org/10.1002/jbmr.499>.
8. Kim BJ, Lee SH, Koh JM. Potential biomarkers to improve the prediction of osteoporotic fractures. *Endocrinol Metab (Seoul).* 2020;35:55–63. <https://doi.org/10.3803/EnM.2020.35.1.55>.
9. Dempster DW, Compston JE, Drezner MK, Glorieux FH, Kanis JA, Malluche H, et al. Standardized nomenclature, symbols, and units for bone histomorphometry: a 2012 update of the report of the ASBMR Histomorphometry Nomenclature Committee. *J Bone Min Res.* 2013;28:2–17. <https://doi.org/10.1002/jbmr.1805>.
10. Brenner AI, Koshy J, Morey J, Lin C, DiPoce J. The bone scan. *Semin Nucl Med.* 2012;42:11–26. <https://doi.org/10.1053/j.semnuclmed.2011.07.005>.
11. Bang J, Park H, Yoo J, Lee D, Choi WI, Lee JH, et al. Selection and identification of a novel bone-targeting peptide for biomedical imaging of bone. *Sci Rep.* 2020;10:10576. <https://doi.org/10.1038/s41598-020-67522-4>.
12. Lee EJ, Kim JY, Park JM, Song BI, Choi H, Shim HK, et al. Computed tomography (CT) protocols Associated with Cardiac and Bone single-Photon Emission

- computed Tomography/CT (SPECT/CT) in Korea. *Nucl Med Mol Imaging*. 2020;54:139–46. <https://doi.org/10.1007/s13139-020-00644-9>.
13. Choi WH, Han EJ, Chang KB, Joo MW. Quantitative SPECT/CT for differentiating between enchondroma and grade I chondrosarcoma. *Sci Rep*. 2020;10:10587. <https://doi.org/10.1038/s41598-020-67506-4>.
 14. Tabotta F, Jreige M, Schaefer N, Becce F, Prior JO, Nicod Lalonde M. Quantitative bone SPECT/CT: high specificity for identification of prostate cancer bone metastases. *BMC Musculoskelet Disord*. 2019;20:619. <https://doi.org/10.1186/s12891-019-3001-6>.
 15. Adams JE. Quantitative computed tomography. *Eur J Radiol*. 2009;71:415–24. <https://doi.org/10.1016/j.ejrad.2009.04.074>.
 16. Schwaiger BJ, Gersing AS, Baum T, Noel PB, Zimmer C, Bauer JS. Bone mineral density values derived from routine lumbar spine multidetector row CT predict osteoporotic vertebral fractures and screw loosening. *AJNR Am J Neuroradiol*. 2014;35:1628–33. <https://doi.org/10.3174/ajnr.A3893>.
 17. Kato S, Demura S, Matsubara H, Inaki A, Shinmura K, Yokogawa N, et al. Utility of bone SPECT/CT to identify the primary cause of pain in elderly patients with degenerative lumbar spine disease. *J Orthop Surg Res*. 2019;14:185. <https://doi.org/10.1186/s13018-019-1236-4>.
 18. Cachovan M, Vija AH, Hornegger J, Kuwert T. Quantification of 99mTc-DPD concentration in the lumbar spine with SPECT/CT. *EJNMMI Res*. 2013;3:45. <https://doi.org/10.1186/2191-219X-3-45>.
 19. Huang K, Feng Y, Liu D, Liang W, Li L. Quantification evaluation of (99m)Tc-MDP concentration in the lumbar spine with SPECT/CT: compare with bone mineral density. *Ann Nucl Med*. 2020;34:136–43. <https://doi.org/10.1007/s12149-019-01425-x>.
 20. Kaneta T, Ogawa M, Daisaki H, Nawata S, Yoshida K, Inoue T. SUV measurement of normal vertebrae using SPECT/CT with Tc-99m methylene diphosphonate. *Am J Nucl Med Mol Imaging*. 2016;6:262–8.
 21. Cifuentes M, Johnson MA, Lewis RD, Heymsfield SB, Chowdhury HA, Modlesky CM, et al. Bone turnover and body weight relationships differ in normal-weight compared with heavier postmenopausal women. *Osteoporos Int*. 2003;14:116–22. <https://doi.org/10.1007/s00198-002-1324-9>.
 22. Wu XY, Li HL, Xie H, Luo XH, Peng YQ, Yuan LQ, et al. Age-related bone turnover markers and osteoporotic risk in native Chinese women. *BMC Endocr Disord*. 2014;14:8. <https://doi.org/10.1186/1472-6823-14-8>.
 23. Frost ML, Cook GJ, Blake GM, Marsden RK, Fogelman I. Dissociation between global markers of bone remodelling and direct measurement of spinal bone formation in osteoporosis. *J Bone Min Res*. 2004;19:5305–5.
 24. Wong KK, Piert M. Dynamic bone imaging with ^{99m}Tc-labeled diphosphonates and ^{18F}-NaF: mechanisms and applications. *J Nucl Med*. 2013;54:590–9. <https://doi.org/10.2967/jnumed.112.114298>.
 25. Rosen H, Lau A, Szalat A, Tanner SB, Krueger D, Prout T, et al. Reporting fewer Than Four Vertebrae: 2023 official positions of the International Society for Clinical Densitometry. *J Clin Densitom*. 2024;27:101436. <https://doi.org/10.1016/j.jocd.2023.101436>.
 26. Faulkner KG. Bone matters: are density increases necessary to reduce fracture risk? *J Bone Min Res*. 2000;15:183–7. <https://doi.org/10.1359/jbmr.2000.15.2.183>.
 27. Frost ML, Compston JE, Goldsmith D, Moore AE, Blake GM, Siddique M, et al. (18F)-fluoride positron emission tomography measurements of regional bone formation in hemodialysis patients with suspected adynamic bone disease. *Calcif Tissue Int*. 2013;93:436–47. <https://doi.org/10.1007/s00223-013-9778-7>.
 28. Segall G, Delbeke D, Stabin MG, Even-Sapir E, Fair J, Sajdak R, et al. SNM Practice Guideline for Sodium ¹⁸F-Fluoride PET/CT bone scans 1.0. *J Nucl Med*. 2010;51:1813–20. <https://doi.org/10.2967/jnumed.110.082263>.
 29. Cvijetic S, Korsic M. Apparent bone mineral density estimated from DXA in healthy men and women. *Osteoporos Int*. 2004;15:295–300. <https://doi.org/10.1007/s00198-003-1525-x>.
 30. Front D, Israel O, Jerushalmi J, Frenkel A, Losilevsky G, Feinsod M, et al. Quantitative bone Scintigraphy using SPECT. *J Nucl Med*. 1989;30:240–50.
 31. Israel O, Gips S, Lubushitzky R, Bettman L, Losilevsky G, Hardoff R, et al. Prediction of bone loss in patients with primary hyperparathyroidism using quantitative bone SPECT. *J Nucl Med*. 1999;39:1614–7.
 32. Huang SC. Anatomy of SUV. *Nucl Med Biol*. 2000;27:643–6.
 33. de Laet CE, van der Klift M, Hofman A, Pols HA. Osteoporosis in men and women: a story about bone mineral density thresholds and hip fracture risk. *J Bone Min Res*. 2002;17:2231–6. <https://doi.org/10.1359/jbmr.2002.17.12.2231>.
 34. Ikegami S, Kamimura M, Nakagawa H, Takahara K, Hashidate H, Uchiyama S, et al. Comparison in bone turnover markers during early healing of femoral neck fracture and trochanteric fracture in elderly patients. *Orthop Rev (Pavia)*. 2009;1:e21. <https://doi.org/10.4081/or.2009.e21>.
 35. Kim H, Kim JH, Kim MJ, Hong AR, Choi H, Ku E, et al. Low predictive value of FRAX adjusted by trabecular bone score for osteoporotic fractures in Korean Women: A Community-based Cohort Study. *Endocrinol Metab (Seoul)*. 2020;35:359–66. <https://doi.org/10.3803/EnM.2020.35.2.359>.
 36. Ravn P, Rix M, Andreassen H, Clemmesen B, Bidstrup M, Gunnes M. High bone turnover is associated with low bone mass and spinal fracture in postmenopausal women. *Calcified Tissue Int*. 1997;60:255–60. <https://doi.org/10.1007/s002239900225>.
 37. Dagan N, Elnekave E, Barda N, Bregman-Amitai O, Bar A, Orlovsky M, et al. Automated opportunistic osteoporotic fracture risk assessment using computed tomography scans to aid in FRAX underutilization. *Nat Med*. 2020;26:77–82. <https://doi.org/10.1038/s41591-019-0720-z>.
 38. Pickhardt PJ, Graffy PM, Zea R, Lee SJ, Liu J, Sandfort V, et al. Automated abdominal CT imaging biomarkers for opportunistic prediction of future major osteoporotic fractures in asymptomatic adults. *Radiology*. 2020;297:64–72. <https://doi.org/10.1148/radiol.2020200466>.
 39. Lee K, Kim H, Kim YI, Park B, Shim WH, Oh JS, et al. Preliminary Study for Quantitative Assessment of Sacroiliitis Activity using bone SPECT/CT: comparison of diagnostic performance of quantitative parameters. *Nucl Med Mol Imaging*. 2022;56:282–90. <https://doi.org/10.1007/s13139-022-00766-2>.
 40. Engelke K, Fuerst T, Dasic G, Davies RY, Genant HK. Regional distribution of spine and hip QCT BMD responses after one year of once-monthly ibandronate in postmenopausal osteoporosis. *Bone*. 2010;46:1626–32. <https://doi.org/10.1016/j.bone.2010.03.003>.

Publisher's Note

Springer Nature remains neutral with regard to jurisdictional claims in published maps and institutional affiliations.